

Improved Water Suppression for Localized *in Vivo* ^1H Spectroscopy

THOMAS ERNST* AND JÜRGEN HENNIG

Department of Radiology, MR Tomography, University Freiburg, Hugstetterstrasse 55, D-79106 Freiburg, Germany

Received May 11, 1994; revised August 4, 1994

The quality of localized proton spectra of the human brain has been greatly improved in the past few years. PRESS (1, 2) and STEAM (3) experiments at short echo times ($TE < 30$ milliseconds) provide a wealth of spectral information, and shielded gradients eliminate artifacts due to eddy currents. However, water suppression has not kept pace with these improvements. Because of the short transverse relaxation time of brain tissue (< 100 milliseconds in adult brain), the residual water signal at short TE is about one order of magnitude larger than that at long TE (135 or 270 ms). Furthermore, current water-suppression schemes are inefficient at suppressing signals from two or more compartments with differing T_1 values, such as brain tissue and cerebrospinal fluid (CSF).

The water-suppression technique most widely used for localized *in vivo* spectroscopy is presaturation with chemical-shift-selective RF pulses (4). The amplitude of the RF pulses is adjusted so that the z magnetization at the start of the localization sequence is zero. Each RF pulse is followed by a spoiler gradient which dephases transverse magnetization. Such a unit of RF pulse and spoiler gradient will be called a CHES cycle throughout this paper. Moonen *et al.* (5) discussed schemes of spoiler gradients by which artifacts due to refocusing of unwanted coherences of the water spins can be minimized. However, this by itself does not guarantee sufficient water suppression. The timing and relative amplitudes of the individual RF pulses are just as crucial.

One of the water-suppression schemes used most frequently comprises three CHES cycles with identical RF amplitudes and equidistant timing. This approach has the problem that the zero-crossing point of the water signal depends on T_1 so that the signals from tissue water and CSF cannot be suppressed simultaneously (6). Another scheme commonly used, with only two CHES cycles and equidistant timing but differing flip angles, has the same drawback. For that reason, a recent paper suggested the application of a double inversion-recovery sequence with three CHES cycles and one long and one short inversion period (7). However, with a total duration of over one second, the sequence is very time consuming and cannot be applied with certain

multivoxel techniques (8). Schemes with four CHES cycles have also been analyzed (9); this seems disadvantageous because each additional RF pulse increases the number of coherence pathways and thus the probability of unwanted echoes (10). The purpose of this paper is to design a water-suppression scheme that uses only three CHES cycles and equidistant or nearly equidistant timing and that results in water-suppression factors greater than 1000 for a wide range of T_1 and flip-angle values.

The pulse sequence of such an experiment is shown in Fig. 1A. Three RF pulses with flip angles α , β , and γ are applied. The intervals between the RF pulses are t_1 and t_2 , while t_3 represents the delay between the third saturation pulse and the start of the localization sequence. The evolution of z magnetization during this sequence was calculated with the Mathematica software (Wolfram Research, Champaign, Illinois). Calculations were done with the assumption that transverse magnetization is completely dephased by the spoiler gradients G , and that T_1 relaxation during the RF pulses can be neglected.

Starting from steady-state magnetization M_s , the longitudinal magnetization M_1 after the first pulse α is

$$M_1 = M_s \cos(\alpha). \quad [1]$$

The effect of T_1 relaxation, during an interval t , on z magnetization M_z can be described by a function "relax (t, M_z),"

$$\text{relax}(t, M_z) = M_0 + (M_z - M_0)\exp(-t/T_1), \quad [2]$$

where M_0 represents the equilibrium magnetization. We can thus write for the z magnetization M_{2-} directly prior to the second RF pulse:

$$M_{2-} = \text{relax}(t_1, M_1) = \text{relax}(t_1, M_s \cos(\alpha)). \quad [3]$$

The magnetization M_{2+} directly after the second RF pulse is

$$M_{2+} = M_{2-} \cos(\beta). \quad [4]$$

By reiterating this scheme, we obtain M_L , the residual z magnetization at the beginning of the localization sequence:

* To whom correspondence should be addressed at Harbor UCLA Medical Center, Department of Neurology, Bldg. F-9, 1000 W. Carson Street, Torrance, California 90509.

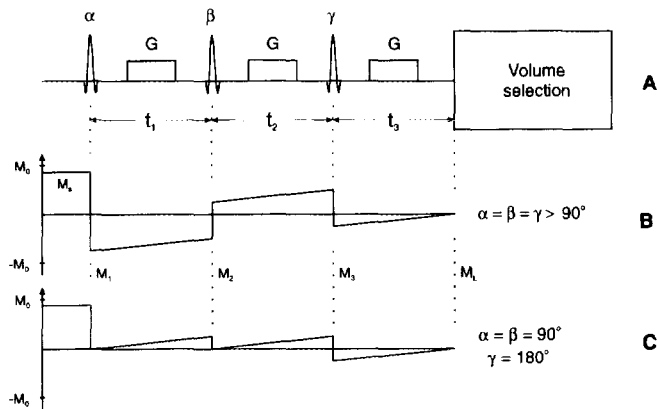


FIG. 1. (A) Timing diagram of a water-suppression sequence comprising three CHES cycles with spoiler gradients G and RF pulses α , β , and γ . The water-suppression sequence is followed by a localized-spectroscopy experiment such as PRESS or STEAM. (B) and (C) show the corresponding evolution of longitudinal magnetization for the flip angles indicated. Water suppression is perfect if the residual z magnetization M_L at the start of the localization sequence is zero.

$$M_L = \text{relax}\{t_3, \cos(\gamma)\} \\ \times \text{relax}[t_2, \cos(\beta) \text{relax}(t_1, \cos(\alpha)M_s)]. \quad [5]$$

Our aim is to find a combination of timing parameters and flip angles that minimizes the dependence of M_L on T_1 and variations in the flip angles. We will examine various schemes with fixed durations and fixed ratios of flip angles, and consider only variations in T_1 and one global flip angle θ . A pulse sequence is characterized by the parameter set $\{t_1, t_2, t_3; \theta, b\theta, g\theta\}$ with the RF scaling factors b and g and $\alpha = \theta$, $\beta = b\theta$, and $\gamma = g\theta$.

The sequence $\{\tau, \tau, \tau; \theta, \theta, \theta\}$, comprising three CHES cycles with identical flip angles ($\alpha = \beta = \gamma = \theta$) and equidistant timing ($t_1 = t_2 = t_3 = \tau$), has been the workhorse of localized *in vivo* ^1H spectroscopy. The evolution of z magnetization during this sequence is shown in Fig. 1B. The flip angles must be above 90° for optimal water suppression, so that the RF pulses act neither as pure saturation nor as pure inversion pulses. The dependence of M_L/M_0 on the global flip angle θ is plotted in Fig. 2 (top, 1-1-1.0). The solid and dashed curves characterize brain tissue ($\tau/T_1 = 0.05$) and CSF ($\tau/T_1 = 0.02$), respectively. The left graph shows the global features for a wide range of flip angles. The z magnetization is slightly positive for $\theta = 90^\circ$, and slowly approaches zero at about 110° . A magnification of the zero-crossing region (Fig. 2, top right) reveals that the zero-crossing points for brain tissue and CSF differ by 6° . The residual z magnetization of one species at the optimum of the other species is more than 2%, a value unacceptable for spectroscopy at short echo times. The slope of M_L at the zero crossing is about $dM_L/d\theta = 4 \times 10^{-3}/1^\circ$, which means the flip angles have to be within 0.25° to achieve suppression factors of 1000:1 for one species.

As an improved version of the experiment with equidistant timing, we suggest the sequence $\{\tau, \tau, \tau; \theta, \theta, 2\theta\}$, in which the last RF pulse is applied with double amplitude ($\alpha = \beta = \theta; \gamma = 2\theta$). The first two RF pulses act as saturation pulses, while the third pulse inverts the z magnetization building up in the t_2 interval (Fig. 1C). For $\tau \ll T_1$, the change of M_z in the t_3 period is very close to that in the t_2 period, so that M_L is very close to zero, independently of T_1 . This is very easy to demonstrate. For $\alpha = \beta = \theta = 90^\circ$, the z magnetization M_{2+} directly after the second RF pulse is zero. The z magnetization M_{3-} building up in the $t_2 = \tau$ interval is

$$M_{3-} = M_0(1 - \exp(-\tau/T_1)). \quad [6]$$

The inversion pulse $\gamma = 2\theta = 180^\circ$ leads to $M_{3+} = -M_{3-}$, so that the longitudinal magnetization M_L after the period $t_3 = \tau$ is

$$M_L = \text{relax}(\tau, -M_{3-}) \quad [7a]$$

or

$$M_L = M_0(1 - \exp(-\tau/T_1))^2, \quad [7b]$$

using Eq. [3]. For $\tau/T_1 \ll 1$, we can approximate

$$M_L \sim M_0(\tau/T_1)^2. \quad [7c]$$

Thus, the longitudinal magnetization of water at the beginning of the localization sequence depends on T_1 only quadratically. Equation [7c] indicates that, with $\tau/T_1 \leq 0.05$, typically, very high suppression factors are achievable. The improved pulse sequence is not only insensitive to T_1 but also to variations in the flip angle. This is quite obvious for the inversion pulse γ because of the second-order behavior of $\cos(\gamma)$ at $\gamma = 180^\circ$. The other major condition for the nulling of M_L is that M_{2+} , the z magnetization directly after the second RF pulse, is zero. It is sensible that this condition can be achieved very effectively by applying two saturation pulses, because neither pulse has a major impact on M_{2+} and thus M_L .

These considerations are confirmed by the numerical simulation displayed in Fig. 2 (bottom, 1-1-2.0). The full-scale plot (bottom left) shows there is a first-order zero-crossing point for $\theta \sim 45^\circ$, when the third pulse $\gamma = 2\theta$ saturates M_z . Increasing the flip angle above this point leads to negative longitudinal magnetization, with a local minimum at $\theta \sim 60^\circ$. In the region of the optimal flip angle ($\theta \sim 90^\circ$), $M_L(\theta)$ is characterized by a local maximum very close to zero, and virtually independent of T_1 . This is supported by the magnification of the zero-crossing region shown on the right side. The zero-crossing point for brain tissue (dashed curve) is within 1° of that of CSF (solid curve). Even more importantly, $|M_L|$ of both CSF and brain tissue

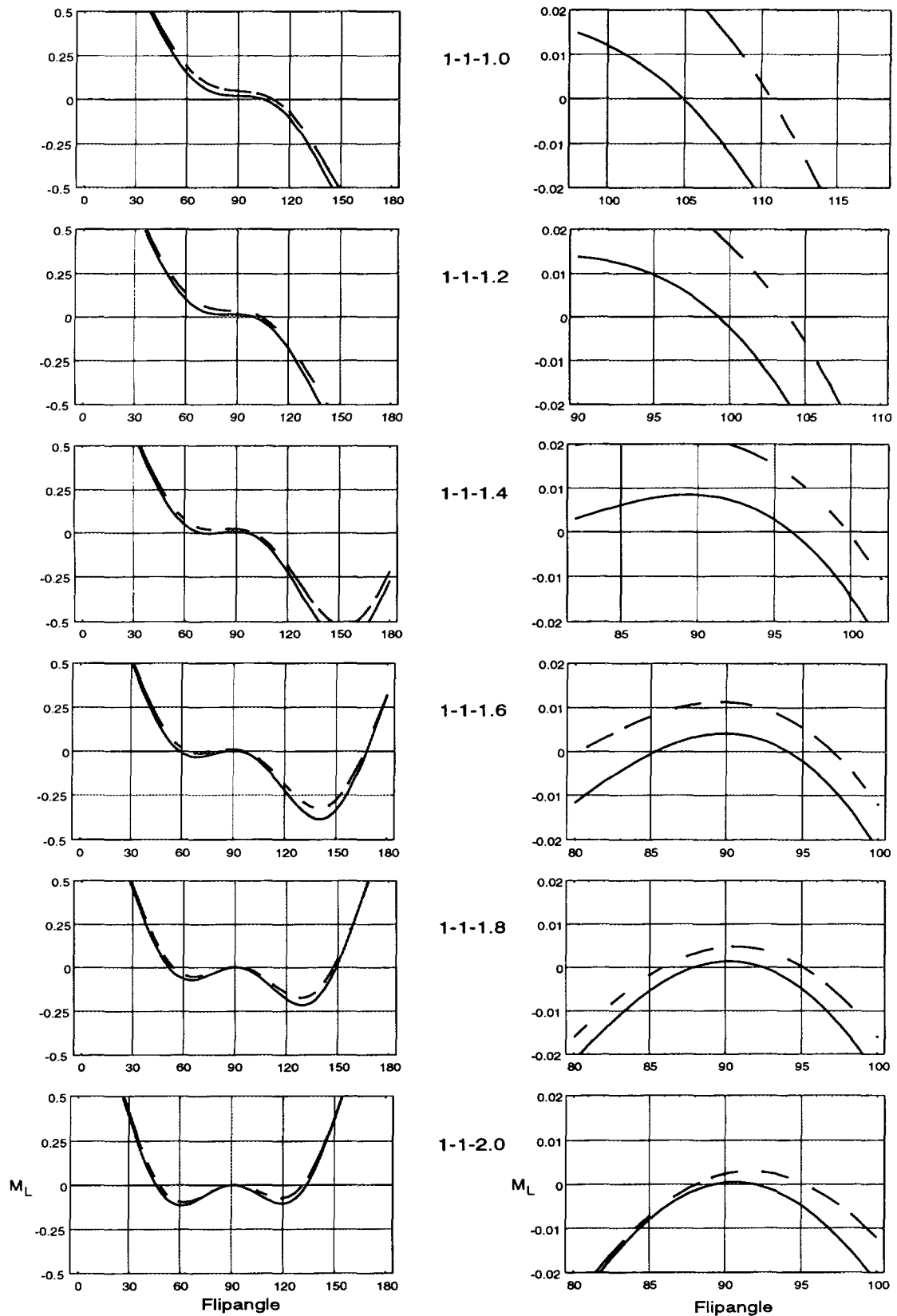


FIG. 2. Simulated flip-angle dependence of M_L , the residual z magnetization at the start of the localization sequence, on the global flip angle θ for water-suppression sequences with three CHES cycles and equidistant timing. The numbers in the center indicate the scaling of α , β , and γ with θ ; i.e., the plots demonstrate the transition from a “conventional” $\{\tau, \tau, \tau; \theta, \theta, \theta\}$ scheme (1-1-1.0) with identical flip angles to the improved $\{\tau, \tau, \tau; \theta, \theta, 2\theta\}$ sequence (1-1-2.0), in which the third RF pulse is applied with double amplitude. The left column displays full-range plots while the right column shows a magnified view of the zero-crossing regions. The solid curves are for CSF ($\tau/T_1 = 0.02$) and the dashed curves for brain tissue ($\tau/T_1 = 0.05$).

is smaller than 3×10^{-3} for a flip-angle range of about 7° . The slope of $M_L(\theta)$ is typically smaller than $1 \times 10^{-3}/1^\circ$.

This analysis raises two interesting questions. First, what is the behavior of $M_L(\theta)$ for "intermediate" sequences of the type $\{\tau, \tau, \tau; \theta, \theta, g\theta\}$ with $1.0 < g < 2.0$? Second, is it possible to improve the $\{\tau, \tau, \tau; \theta, \theta, 2\theta\}$ sequence further by fine tuning the timing parameters and flip-angle ratios?

The gross features of sequences of this type are shown in Fig. 2 (left column). For $g > 1.4$, $M_L(\theta)$ exhibits two local minima (one below and one above $\theta = 90^\circ$) and a local maximum at $\theta \sim 90^\circ$. With increasing g , the curves become more symmetric. Simultaneously, the local maxima for brain tissue (dashed) and CSF (solid) approach zero (Fig. 2, right column). Without adjusting the other free parameters, the case $g = 2.0$ leads to optimal results. We note, however (Fig. 2, bottom right), that $g = 2.0$ is not completely satisfactory. Due to a slight asymmetry, the z magnetization of brain tissue is larger than that of CSF, and the positions of the two maxima differ by about 2° . This reduces the range of flip angles yielding sufficient water suppression. Figure 2 also demonstrates that the asymmetry is reduced for $1.6 < g < 1.8$; unfortunately, there is a difference in the residual z magnetization of brain tissue and CSF for these g values. However, these imperfections can be overcome by fine tuning the parameters.

The best sequence with three CHESS cycles and close to equidistant timing we were able to design is the $\{\tau, \tau, 0.87\tau; \theta, 0.94\theta, 1.65\theta\}$ sequence. The plot of $M_L(\theta)$ close to the optimum is given in Fig. 3A, the y axis covering a range of $\pm 4 \times 10^{-3}$ only. The two curves for CSF and brain tissue are nearly coincident and exhibit their maximum at the same flip angle. Due to this symmetry, the residual z magnetization is smaller than 10^{-3} over a range of 7° . Also, the sequence is very insensitive to the starting value M_s of the z magnetization (Fig. 3B). Figure 3C shows that suppression factors of over 1000 can be obtained for relaxation rates τ/T_1 between 0 and 0.075, corresponding to T_1 values between 500 ms and infinity for $\tau = 40$ ms.

In order to verify the theoretical results, we measured the flip-angle dependence of the water signal in a phantom ($T_1 = 3.0$ s). Experiments were performed on a 2T whole-body system with shielded gradients (S200 Bruker, Karlsruhe, FRG) using a standard head resonator. The strength of the spoiler gradients for the CHESS cycles was 10 mT/m. The first two gradients were applied for 15 ms (in the x and y directions, respectively), while the third spoiler gradient was applied for 25 ms (simultaneously in the x and y directions). The interpulse delays were $t_1 = t_2 = t_3 = \tau = 125$ ms. Figure 4 shows there is very good agreement between the measurements and the theoretical curves; the slight differences are most likely caused by nonlinearities of the RF modulator. With the $\{\tau, \tau, \tau; \theta, \theta, \theta\}$ sequence, the data demonstrate the considerable slope of $M_L(\theta)$ at the zero crossing (Fig. 4, top right, 1-1-1). The experiment also reproduces the cur-

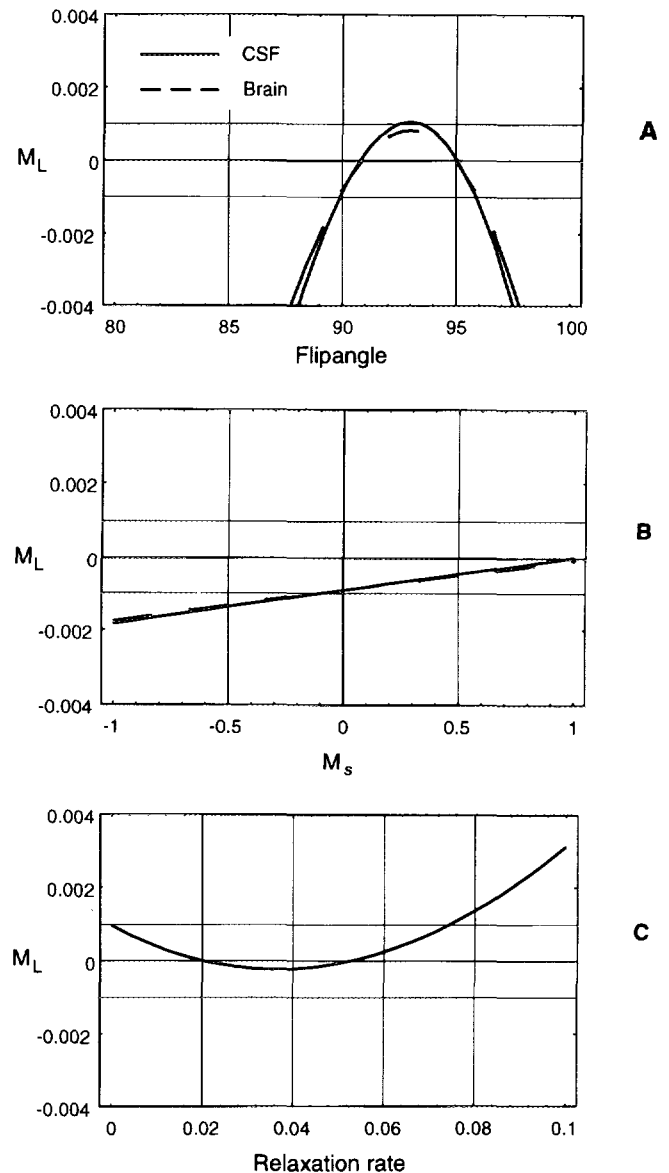


FIG. 3. Simulated behavior of the $\{\tau, \tau, 0.87\tau; \theta, 0.94\theta, 1.65\theta\}$ sequence, numerically optimized for $\tau/T_1 = 0.02$ for CSF (solid curves) and 0.05 for brain tissue (dashed curves). The plots show the dependence of the residual z magnetization M_L on (A) the global flip angle θ , (B) the steady-state magnetization M_s , and (C) the relaxation rate for the flip angle leading to zero crossing of CSF and brain tissue. The y axes are strongly enlarged. The horizontal lines at $M_L = \pm 0.001$ indicate the range where water suppression is sufficient ($>1000:1$) for acquisition of high-quality *in vivo* ^1H spectra.

vature and residual z magnetization calculated for the $\{\tau, \tau, \tau; \theta, \theta, 2\theta\}$ sequence (bottom right, 1-1-2).

Figure 5 displays the results of *in vivo* measurements in a volunteer. Gaussian pulses of 25 ms were used for water suppression, leading to an interpulse delay τ of 44 ms. About 20% of the $(2.5 \text{ cm})^3$ voxel was in the ventricles, a problem occurring rather frequently in older patients with cortical atrophy. With the conventional $\{\tau, \tau, \tau; \theta, \theta, \theta\}$ sequence, it is not possible to simultaneously suppress the contributions

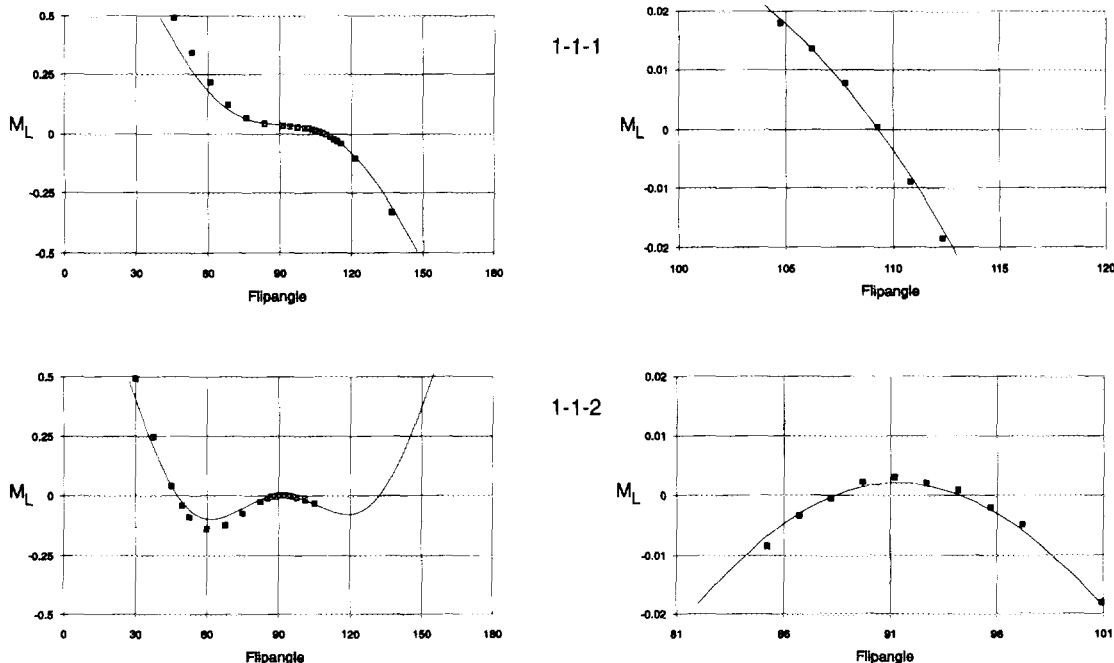


FIG. 4. Comparison of simulated flip-angle dependence of M_L (curves) with experimental data (squares) for the conventional $\{\tau, \tau, \tau; \theta, \theta, \theta\}$ sequence (top, 1-1-1) and the improved $\{\tau, \tau, \tau; \theta, \theta, 2\theta\}$ sequence (bottom, 1-1-2). Experiments were performed in distilled water ($T_1 = 3.0$ s). The theoretical curves were calculated with a relaxation rate of $\tau/T_1 = 0.0417$, corresponding to the experimental value of 125 ms for τ . The left column displays full-range plots, while the right column shows a magnified view of the zero-crossing regions. The experimental RF amplitudes were scaled linearly such that the simulated and experimental zero-crossing points coincide.

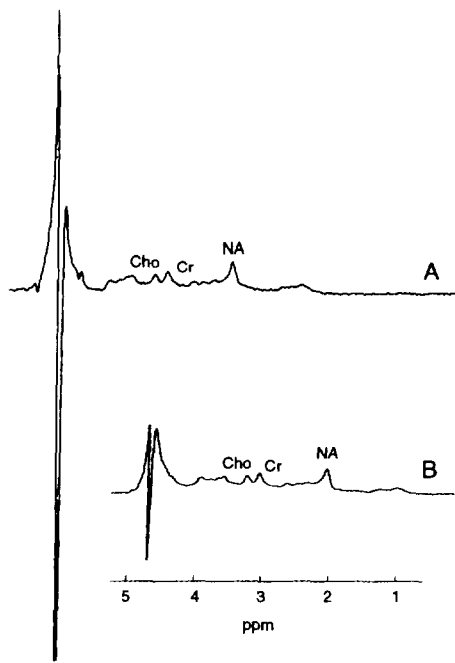


FIG. 5. Localized *in vivo* ^1H spectra of the human brain acquired using (A) the conventional $\{\tau, \tau, \tau; \theta, \theta, \theta\}$ and (B) the improved $\{\tau, \tau, \tau; \theta, \theta, 2\theta\}$ sequence for water suppression. Spectra were acquired with PRESS with $TE = 30$ ms and $TR = 1500$ ms (256 averages). About 20% of the $(2.5\text{ cm})^3$ volume covered the ventricles. Spectrum (A) demonstrates the difficulty of the conventional sequence in simultaneously suppressing CSF and brain tissue. There is a fivefold improvement of water suppression when the $\{\tau, \tau, \tau; \theta, \theta, 2\theta\}$ sequence is applied (B).

from CSF and brain tissue (Fig. 5A) so that the spectrum is dominated by the residual water resonance. While the broader component of the residual water (from brain tissue) is positive compared to the metabolites, the narrower component (from CSF) is inverted. Any attempt to improve the suppression of one component deteriorates suppression of

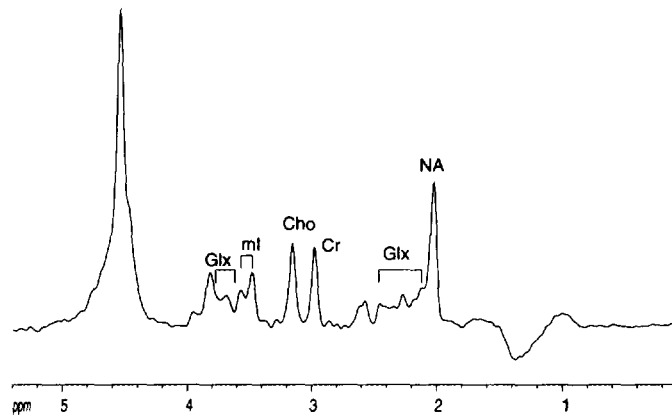


FIG. 6. Localized *in vivo* ^1H spectrum of the human brain acquired with the $\{\tau, \tau, \tau; \theta, \theta, 2\theta\}$ sequence for water suppression. A PRESS sequence with $TE = 30$ ms and $TR = 1500$ ms was applied (256 averages). In contrast to Fig. 5, the partial volume of CSF is negligible in this case. By using the *N*-acetyl (NA) resonance as concentration reference (10 mM), the water-suppression factor can be estimated to be approximately 1500:1. Cr, total creatine; Cho, choline; ml, *myo*-inositol; Glx, glutamate and glutamine.

the other component. By using the *N*-acetyl (NA) resonance as reference (10 mM), the water-suppression factor can be estimated to be approximately 200:1. Such a factor is expected from Fig. 2 (top right) if the partial volume of CSF is taken into account. With suppression factors of about 1000:1 for both compartments, the situation is considerably improved when the $\{\tau, \tau, \tau; \theta, \theta, 2\theta\}$ sequence is applied to acquire the proton spectrum of the same voxel (Fig. 5B). Figure 6 gives an example of what can be achieved if the partial volume of CSF is negligible. The water signal is suppressed 1500-fold now, and its height is comparable to that of the cerebral metabolites.

In conclusion, the major requirements for water suppression in localized ^1H spectroscopy at short echo times are insensitivity to relaxation time and flip angle, suppression factors over 1000, and economical use of RF pulses and time. Compared to the standard $\{\tau, \tau, \tau; \theta, \theta, \theta\}$ scheme, the $\{\tau, \tau, \tau; \theta, \theta, 2\theta\}$ sequence leads to a fivefold improvement in water suppression. The installation of this sequence is straightforward if the standard sequence with identical flip angles and equidistant timing is already used. Of all sequences presented in this paper, the $\{\tau, \tau, 0.87 \tau; \theta, 0.94 \theta, 1.65 \theta\}$ parameter set is the most insensitive to variations in the flip

angle and in T_1 . This sequence should therefore be ideal for ^1H chemical-shift imaging (11, 12) at short echo times.

REFERENCES

1. P. A. Bottomley, *Ann. N.Y. Acad. Sci.* **508**, 333 (1987).
2. R. J. Ordridge, M. R. Bendall, R. E. Gordon, and A. Conolly, in "Magnetic Resonance in Biology and Medicine," pp. 387-397, Govil, Khetrapal, Saran, 1985.
3. J. Frahm, K. D. Merboldt, and W. Hänicke, *J. Magn. Reson.* **72**, 502 (1987).
4. A. Haase, J. Frahm, W. Hänicke, and D. Matthei, *Phys. Med. Biol.* **30**, 341 (1985).
5. C. T. W. Moonen and P. C. M. van Zijl, *J. Magn. Reson.* **88**, 28 (1990).
6. R. J. Ogg, P. B. Kingsley, and J. S. Taylor, *Abstracts of the Society of Magnetic Resonance in Medicine*, p. 2134, 1992.
7. J. Shen and J. K. Saunders, *Magn. Reson. Med.* **29**, 540 (1993).
8. Th. Ernst and J. Hennig, *Magn. Reson. Med.* **20**, 27 (1991).
9. J. B. Murdoch and D. A. Lampman, *Abstracts of the Society of Magnetic Resonance in Medicine*, p. 1191, 1993.
10. J. Hennig, *Concepts Magn. Reson.* **3**, 125 (1991).
11. T. R. Brown, B. M. Kincaid, and K. Ugurbil, *Proc. Natl. Acad. Sci. USA* **79**, 3523 (1982).
12. A. A. Maudsley, *J. Magn. Reson.* **68**, 363 (1986).